

COVER SHEET

*NOTE: This coversheet is intended for you to list your article title and author(s) name only
—this page will not print with your article.*

*Title: Detection and Evaluation of Impact Damage on Aircraft Control Surface Using
Acoustic Emission and Convolution Neural Network*

Authors: Li Ai

Elhussien Elbatanouny

Laxman K C

Mahmoud Bayat

Vafa Soltangharaei

Michel van Tooren

Paul Ziehl

Li Ai, Department of Civil and Environmental Engineering, University of South Carolina, Columbia, SC 29201, USA

Elhussien Elbatanouny, Department of Civil and Environmental Engineering, University of South Carolina, Columbia, SC 29201, USA

Laxman K C, Department of Civil and Environmental Engineering, University of South Carolina, Columbia, SC 29201, USA

Mahmoud Bayat, Department of Civil and Environmental Engineering, University of South Carolina, Columbia, SC 29201, USA

Vafa Soltangharaei, Department of Civil and Environmental Engineering, University of South Carolina, Columbia, SC 29201, USA

Michel van Tooren, Department of Civil and Environmental Engineering, University of South Carolina, Columbia, SC 29201, USA

Paul Ziehl, Department of Civil and Environmental Engineering, University of South Carolina, Columbia, SC 29201, USA

ABSTRACT

Impact damage is one of the major threats to the integrity of aircraft control surfaces such as wings and elevators. The conventional and widely applied inspection approach is visual inspection which is time-consuming and subject to human error. The innovation of this paper lies in developing a smart sensing system by leveraging acoustic emission (AE) for the real-time detection and evaluation of impact damage on aircraft elevators. The challenge of this system is to deploy a minimal number of AE sensors on the aircraft due to the environmental restriction during the operation of the aircraft while still effectively evaluate the impact damage. A convolutional neural network (CNN) is employed to localize the impact and evaluate the damage level by analyzing the wavelet of signals obtained by a single AE sensor. The proposed approach is verified by an impact test carried out on a thermoplastic aircraft elevator. The results demonstrate the efficacy and potential of the proposed approach.

INTRODUCTION

One of the most serious risks to the structural integrity of composite aircraft components is in-flight impact damage. Impact damage is usually assessed by traditional visual assessment. However, this approach takes time and is due to human error. Due to recent advances in sensor technology and data processing methods, structural health monitoring systems can now be used to automatically locate impact and assess the damage. This can be used in conjunction with, or as a partial substitute for, manually visual inspection.

Acoustic emission (AE) is a structural health monitoring technique that is highly sensitive to material damage initiation and propagation [1]. Previous research [2-3] has looked into the use of AE monitoring for fiber composite materials. Eaton et al. [2] used AE to study damage characterization in composite materials. The amplitude ratio (MAR) of the two principal Lamb wave modes has been established as a method for damage characterization. Shahri et al. [3] used AE to assess the damage of composite materials. The authors devised an approach based on the Hilbert transform to correlate AE signals to their associated failure mechanisms.

The application of AE for evaluating the impact on fiber composite materials has also been examined [4-5]. Mal et al. [4] applied AE to graphite-epoxy composite plates to detect low-velocity impacts. To gain thorough information on the link between the impact load and the signals, the response of the plate was approached using a modified lamination theory. The findings showed that the impact loading could be identified simply from AE signals, and delamination damage may be assessed by examining the waveforms of the recorded AE signals. Saeedifar et al. [5] used several AE sensors to monitor impact damage in carbon epoxy laminates during quasi-static indentation and low-velocity impact. The authors claimed that AE is an effective method for detecting the barely visible.

According to the investigations mentioned above, AE monitoring of the impact on fiber composite materials is promising. However, due to environmental restrictions during aircraft operation, the issue of applying this approach to aircraft is to put a small number of AE sensors (i.e., a single AE sensor) on the aircraft while still

properly evaluating impact damage. Machine learning techniques could be a viable option for resolving the issue. Artificial neural networks (ANN) and random forests have been used to localize impact events on aircraft components[6-7]. Soltangharaei et al. [6] designed a system to localize impacts on aircraft components using a single AE sensor. An ANN model was employed using AE features as inputs, and the source localization results were produced as outputs. The results showed that impact localization utilizing AE and ANN could achieve respectable results while adhering to weight and power constraints. In a later study, Ai et al. [7] further employed a random forest technique to study the single sensor impact localization on aircraft components. The results suggest that random forest may be able to achieve more significant localization than ANN. However, one issue with applying machine learning approaches in evaluating aircraft components is that manually selecting feature is required. The selection of acceptable features primarily relied on prior experience and was challenging, particularly for complicated data sets.

Adopting deep learning may be an option to resolve the issue. Deep learning has the advantage of using raw data as an input set rather than the derived features [8]. Therefore, feature extraction and feature selection are not required. In recent years, deep learning has been applied in the fields of AE monitoring. Shevchik et al. [9] developed an on-site quality monitoring system for additive manufacturing using acoustic emission technologies. A spectral convolutional neural network-based AE data classification approach was proposed. These findings show that deep learning has the potential to improve AE monitoring. In previous research, deep learning was also applied in the localization of impact on aircraft components [10]. A passive structural health monitoring system for aircraft elevators was proposed. A stacked autoencoder neural network was employed to localize the AE signals caused by impacts. However, these works only focused on impact localization, while the identification of impact damage was not investigated.

The identification of impact energy levels was investigated in this paper. The AE signals caused by the impacts with two different impact energies were recorded. An analysis framework was proposed to evaluate the impact energy level and localize the impact by leveraging continuous wavelets transform (CWT) and convolutional neural network (CNN).

IMPACT DETECTION AND ANALYSIS FRAMEWORK

The identification and evaluation framework of impact on control surface includes the in-flight stage and after-flight stage. AE signals are recorded by a single AE sensor and saved as time series in the signal storage during the in-flight stage. After the operation of the aircraft is finished, the storage signals could be downloaded and processed in the after-flight stage. In this paper, the evaluation and localization of impact of elevator control surface are based on AE, continuous wavelets transform (CWT), and convolutional neural network (CNN). CWT is utilized to extract time-frequency features and convert the time series AE waveforms into RGB images. A CNN model is employed to identify the energy level of the impacts. Once finished, the signals in each impact level are assigned to another CNN model to acquire the locations of the impact. The different procedures of the in-flight/after-flight stages are presented in Figure 1.

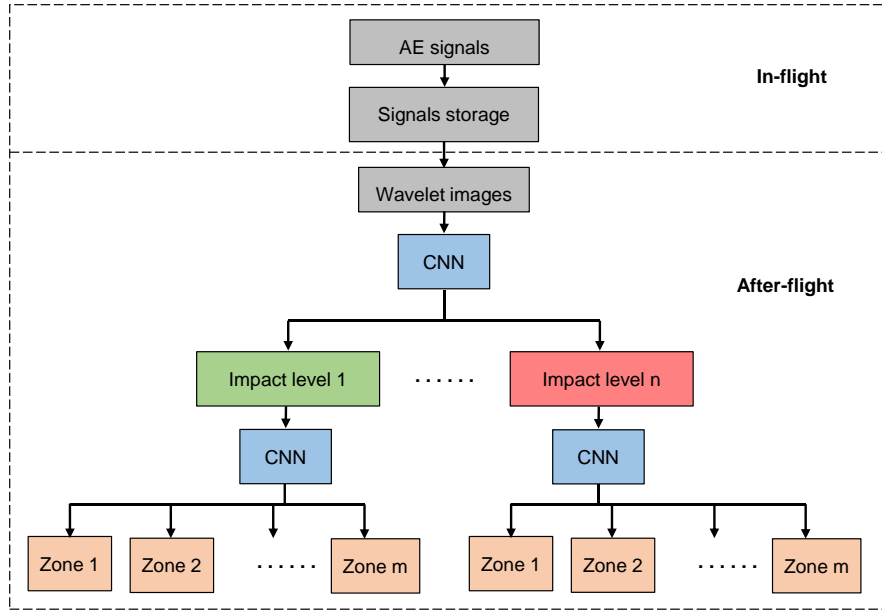


Figure 1. Framework of impact detection and analysis

Wavelet Transform

Continuous wavelets transform (CWT) captures the time-frequency properties of non-stationary signals, such as AE signals. The Morse wavelet is used as the mother wavelet function in this paper to conduct CWT. Eq (1) shows the Fourier transform of a Morse wavelet:

$$\Psi_{p,\gamma}(x) = U(x)\alpha_{p,\gamma}x^{\frac{p^2}{\gamma}}e^{-x^\gamma} \quad (1)$$

where $U(x)$ denotes the unit step, $\alpha_{p,\gamma}$ denotes the normalizing constant, and p^2 is the time-bandwidth product, γ is the parameter that describes the Morse wavelet's symmetry[11]. p^2 and γ was defined as 60 and 3 in this paper

The continuous wavelet coefficients can be expressed using a scalogram image. CNN models use the 2D scalogram pictures as input. The wavelet coefficients are scaled from 0 to 1 in this work.

Convolutional Neural Network

A convolutional neural network (CNN) is a deep neural network containing convolutional filters [12]. The input layer, the feature extraction layers, and the fully connected layer are the three primary parts of a CNN model. The essential part of the feature extraction layers mainly includes convolutional layers and pooling layers. Figure 2 depicts the architecture of a typical CNN with two convolutional layers and two pooling layers.

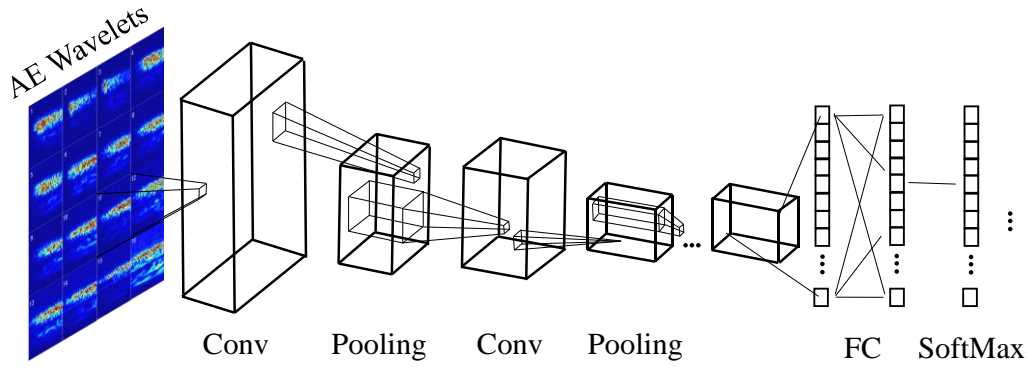


Figure 2. Architecture of a typical CNN

In this study, the input dataset is the aforementioned wavelet images dataset. Before input datasets, the data is labeled and normalized. Since the AE signals available for training in this study are limited, transfer learning based on a pre-trained CNN model is utilized to obtain a more robust neural network, in the meantime, minimizing the required time for training. The pre-trained CNN model employed in this paper is GoogLeNet. The GoogLeNet model is pre-trained by more than a million images. In this paper, the low-level layers are freeze because those layers extract the general features of images. While the rest of the layers could learn the specific feature that is more sensitive to the training data and corresponding labels, the weights of the rest layers are kept not to be frozen. Fine-tuning a pre-trained GoogLeNet model with transfer learning usually leads to a shorter computing time than training from scratch

IMPACT EXPERIMENT

A thermoplastic elevator specimen was utilized in this paper to conduct the impact experiment. The elevator is composed of 20 ribs and 20 thermoplastic panels. Figure 4 illustrates the plane view of the specimen. Two steel balls with varying diameters (0.006 and 0.013 meters) were used to impact the elevator specimen to simulate varied impact levels that the elevator experienced during the flight. The dropping heights were 0.61 meters for both steel balls.

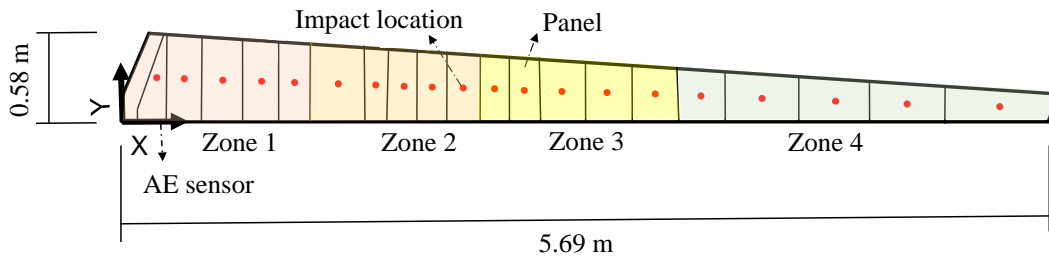


Figure 3. Impact and sensor locations

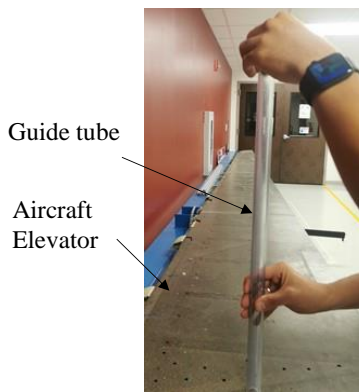


Figure 4. Steel sphere impact procedure

A plastic guide tube was used to keep the impact locations and the dropping heights constantly during the experiment (Figure 4). 0.006 J and 0.05 J are the impact energies of two steel balls. In this paper, they are referred to as impact levels 1 and 2. Figure 4 shows the impact site on each thermoplastic panel as a red dot. The steel balls impacted each dot 60 times. In the meantime, A single AE sensor was attached to the front spar of the elevator to monitor the impacts and record the AE signals. In total, 2,400 AE signals were recorded (1,200 for level 1, and 1,200 for level 2). This paper considered impact localization as a classification task. Panels 1 to 5 were defined as zone 1, Panels 6 to 10 were defined as zone 2, Panels 11 through 15 were defined as zone 3, and panels 16 through 20 were zone 4. The CNN model will classify the input AE signals into their corresponding zones.

The hardware of the AE system was produced by the Mistras Group Inc., Princeton Junction, New Jersey. The AE sensor utilized in this experiment is type PAC Micro-30 with an operating frequency range of 150 - 400 kHz. AE signals were acquired by a 16-channel DiSP system. The pre-trigger time, which recovers AE waveforms before the threshold crossing, was defined as 256 μ s. The sampling rate was 5MHz. The signal length was 2,048 microseconds. The peak definition time (PDT), which refers to the time between the first threshold crossing to the peak amplitude, was defined as 200 μ s, and the hit definition time (HDT) was set to 400 μ s. This controls the stop point of recording and is usually twice the peak definition time [44]. The hit lockout time (HLT), which prevents recording late-arriving signals and reflected hits, was set to 400 μ s.

RESULTS

Because the AE signals acquisition sampling rate was set to 1 MHz and the length was set to 2,048 microseconds, each signal is a time series with 2,048 sample points. The amplitude of all AE signals was normalized to a range of -1 to 1. Figure 4 shows the waveforms of the normalized signals that were randomly selected from each zone. The patterns of the AE waveforms in different zones can be seen to be distinct. In addition, as illustrated in Figure 4, the AE waveforms were used to construct CWT coefficients. The CWT coefficient's Y-axis was then transformed to a logarithmic coordinate to display the time-frequency component better. The coefficients were

stored as RGB pictures of $224 \times 224 \times 3$ pixels in size (Figure 4). The resulting RGB images were used as the input to the CNN model in the CWT image-based dataset.

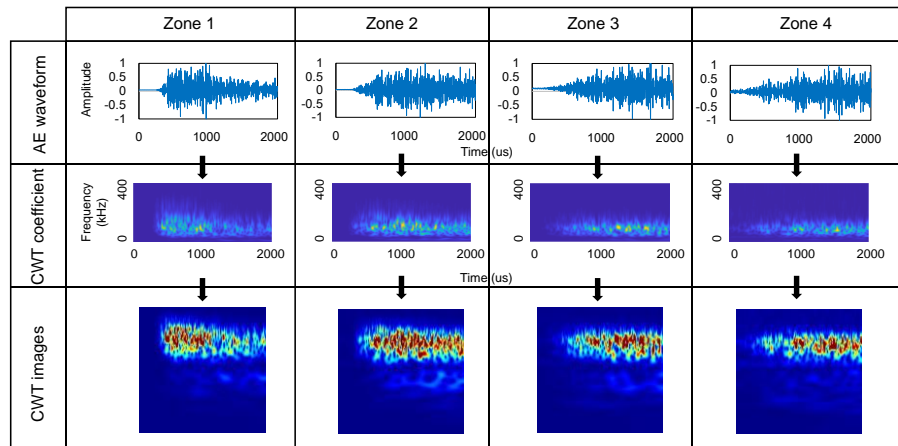


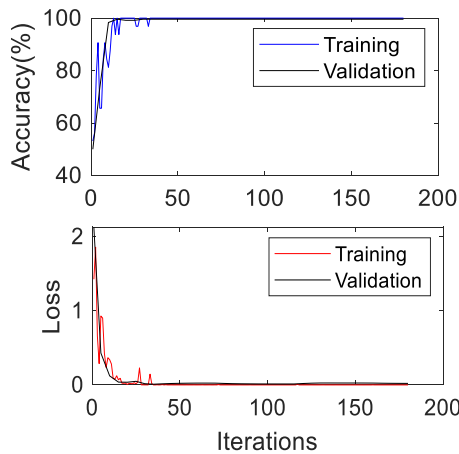
Figure 5. AE waveforms, CWT coefficient, and CWT RGB images

After the 2400 AE signals are converted to RGB images, they are assigned to a CNN model to identify the impact level. 60% of the images (1440 images) were randomly selected as a training set. 10% (240 images) was selected as a validation set. The resting 30% (720 images) of the images were utilized as a testing set. The optimizer of the CNN model was the Adaptive moment estimation (Adam) method. The batch size was 16, the learning rate was 0.0001, and the maximum epochs was 4. Figures 6a and 6b present the accuracy and loss curves of the training and validation. The training accuracy reached 100%, and the accuracy of training reached 99.72% accuracy by the end of iteration 180. Both the losses of training and validation were close to 0 in the end. The training and validation reached convergence around iteration 40, and the curves were stable after converging. The testing results are presented in Figure 6 as a confusion matrix. The accuracy for the impact level identification is 99.9%. All signals of level-I were correctly identified. 399 signals of level 2 were successfully identified. Only one were identified to level 2 by error.

After the impact level was identified, the AE wavelets images of each impact level were transferred to another CNN model to conduct the source localization. The ratio of training/validation/testing was keeping the same as above. The optimizer of the CNN model was the Adaptive moment estimation (Adam) method. The batch size was 32, the learning rate was 0.0001, and the maximum epochs were 17 for the localization of level 1 impacts and 15 for the localization of level 2 impacts. For the impacts of level 1, the localization results are shown in the confusion matrix (Figure 7a). The accuracy is 97.8%. Among tall the 90 signals in zone 1, all signals were correctly localized. In zone 2, 86 signals were successfully localized. One signal was localized to zone 1, and the other 3 were located to zone 3 by mistake. In zone 3, 88 signals were successfully localized, one was localized to zone 1, one was located to zone 4 by error. 88 signals in zone 4 were located to the correct zone, two signals were localized to zone 3 by error.

For the impacts of level 2, 354 AE signals were correctly located out of the 360 test signals, and the localization accuracy is 98.3% (Figure 6b). 89 signals in zone 1 were correctly localized to zone 1, and one was located to zone 2. In zone 2, 86 signals were successfully localized, three signal was localized to zone 1, one was located to

zone 3 by mistake. In zone 3, all signals were correctly localized. In zone 4, 89 signals were located correctly, and the other one was localized to zone 3 by error.



(a)

				Recall
Actual Label	Level1	360	0	100%
	Level2	1	359	99.7%
Precision		99.7%	100%	Accuracy 99.9%
		Level 1	Level 2	

Evaluation Output

(b)

Figure 6. Impact level identification results: (a) training and validation curves; (b) impact level identification

				Recall		
Actual Label	Zone1	90	0	0	0	100%
	Zone2	1	86	3	0	100%
	Zone3	0	1	88	1	100%
	Zone4	0	0	2	88	100%
Precision		100%	100%	100%	100%	Accuracy 97.8%
		Zone1	Zone2	Zone3	Zone4	

Evaluation Output

(a)

				Recall		
Actual Label	Zone1	89	1	0	0	100%
	Zone2	3	86	1	0	90.9%
	Zone3	0	0	90	0	100%
	Zone4	0	0	1	89	100%
Precision		90.0%	100%	100%	100%	Accuracy 98.3%
		Zone1	Zone2	Zone3	Zone4	

Evaluation Output

(b)

Figure 6. Localization results: (a) impact localization of impact level 1; (b) impact localization of impact level 2

CONCLUSIONS

In this paper, The AE signals of two impact energies (impact level 1 and level 2) were collected by conducting an impact experiment using steel balls with two different diameters. An analysis framework to evaluate the impact energy level and localize the impact was proposed by leveraging CNN models. By utilizing AE monitoring and CNN, A good performance (99.9%) on the impact level identification can be observed. The CNN models could also accomplish the impact localization with high accuracy when a single AE sensor is used. Comparing the localization results of the impact of

energy level 1 and level 2, the impact with higher energy could acquire a higher localization accuracy (98.3%) than the impact with lower energy (97.8%).

REFERENCES

1. Ono, K. 2018. "Review on Structural Health Evaluation with Acoustic Emission,". *Applied Sciences*. 8(6):958.
2. Eaton, M., May, M., Featherston, C., Holford, k., Hallet, S., and Pullin, R. 2011. "Characterization of Damage in Composite Structures using Acoustic Emission,". *Journal of Physics: Conference Series*, vol. 305, no. 1, p. 012086.
3. Shahri, M., Yousefi, J., Fotouhi, M and Najfabadi, M. 2016. "Damage evaluation of composite materials using acoustic emission features and Hilbert transform," *Journal of Composite Materials*. 50(14):1897-907.
4. Mal, K., Shih, F and Banerjee, S. 2003. "Acoustic emission waveforms in composite laminates under low velocity impact," *Smart Nondestructive Evaluation and Health Monitoring of Structural and Biological Systems II*. Vol. 5047, pp, 1-122003.
5. Saeedifar, M., Najafabadi, A., Zarouchas, D., Toudeshky, H and Jalalvand, M. 2018. "Barely Visible Impact Damage Assessment in Laminated Composites using Acoustic Emission," *Composites Part B: Engineering*, 152, 180-192.
6. Soltangharaei, V., Anay, R., Begrajka, D., Bijman, M., ElBatanouny, M., Ziehl, P and Van Tooren, M. 2019. "A minimally Invasive Impact Event Detection System for Aircraft Movables," *AIAA Scitech 2019 Forum* (p. 1268).
7. Ai, L., Soltangharaei, V., de Backer, W., Ziehl, P and van Tooren, M. 2020. "A Minimally Intrusive Impact Detection System for Aircraft Moveable using Random Forest," 2020 *The Composites and Advanced Materials Expo*.
8. Ai, L., Soltangharaei, V and Ziehl, P. 2021. "Evaluation of ASR in concrete using acoustic emission and deep learning," *Nuclear Engineering and Design*, 380, 111328.
9. Shevchik, SA., Saeidi, F., Meylan, B and Wasmer, K. 2016. "Prediction of failure in lubricated surfaces using acoustic time–frequency features and random forest algorithm," *IEEE Transactions on Industrial Informatics*. 13(4):1541-53.
10. Ai, L., Soltangharaei, V., Bayat, M., Van Tooren, M. and Ziehl, P. 2021. "Detection of impact on aircraft composite structure using machine learning techniques," *Measurement Science and Technology*, 32(8), p.084013.
11. Lilly, J. M and Olhede, S. C. 2008. "Higher-order properties of analytic wavelets," *IEEE Transactions on Signal Processing*. 57(1), 146-160.
12. Krizhevsky, A., Sutskever, I and Hinton, G. E. 2012. "Imagenet classification with deep convolutional neural networks," *Advances in neural information processing systems*, 25, pp.1097-1105.

IMPORTANT NOTES

1. Your paper should be typed or printed single-spaced, and you should adhere strictly to the margins outlined in the section on "Printing/Typing Your Manuscript." Stay within all margin lines, but fill the page as closely to the margins as possible.
2. DO NOT use San Serif font or Italic faces for the main body of the text.
3. If you create your paper in a program other than MS Word please supply the electronic file as a PDF.
4. If a graph or table must be turned sideways for viewing, please be certain that the top of the table is on the left of the page. There also should not be any text on a page that has a graph or table turned sideways.
5. Questions regarding format should be addressed to Tony Deraco or Steve Spangler, DEStech Publications, Inc.; tel.: 717/290-1660; fax: 717/509-6100; e-mail: aderaco@destechpub.com or sspangler@destechpub.com.
6. For content questions, contact the committee chairperson or the person to whom you should forward Inquiries to.